ID Design Press, Skopje, Republic of Macedonia
Open Access Macedonian Journal of Medical Sciences. 2019 Sep 15; 7(17):2739-2750.
https://doi.org/10.3889/oamjms.2019.730
eISSN: 1857-9655
Basic Science

Combination of Human Amniotic Fluid Derived-Mesenchymal Stem Cells and Nano-hydroxyapatite Scaffold Enhances Bone Regeneration

Eman E. A. Mohammed[1,2*], Hanan H. Beherei[3], Mohamed El-Zawahry[4], Abdel Razik H. Farrag[5], Naglaa Kholoussi[6], Iman Helwa[6], Khaled Gaber[7], Mousa A. Allam[8], Mostafa Mabrouk[3], Alice K. Abdel Aleem[1,2, 9]

[1]Medical Molecular Genetics Department, National Research Centre, Cairo, Egypt; [2]Stem Cell Research Group, Medical Research Centre of Excellence, National Research Centre, Cairo, Egypt; [3]Ceramic Department (Biomaterials), National Research Centre, Cairo, Egypt; [4]Fixed and Removable Prosthodontics Department, National Research Centre, Cairo, Egypt; [5]Pathology Departments, National Research Centre, Cairo, Egypt; [6]Immunogenetics Department, National Research Centre, Cairo, Egypt; [7]Prenatal and Fetal medicine Department, National Research Centre, Cairo, Egypt; [8]Spectroscopy Department, National Research Centre, Cairo, Egypt; [9]Neurology and Neuroscience Department, Weill Cornell Medical College, Doha, Qatar

Citation: Mohammed EEA, Beherei HH, El-Zawahry M, Farrag ARH, Kholoussi N, Helwa I, Gaber K, Allam MA, Mabrouk M, Abdel Aleem AK. Combination of Human Amniotic Fluid Derived-Mesenchymal Stem Cells and Nano-hydroxyapatite Scaffold Enhances Bone Regeneration. Open Access Maced J Med Sci. 2019 Sep 15; 7(17):2739-2750. https://doi.org/10.3889/oamjms.2019.730

Keywords: Amniotic Fluid Stem Cells; 3D Scaffolds; Nano-hydroxyapatite Chitosan; Bone Healing; Bone Regeneration

***Correspondence:** Eman E. A. Mohammed. Medical Molecular Genetics Department, Human Genetics and Genome Research Division, Stem Cell Research Group, Medical Research Centre of Excellence, National Research Centre, Cairo, Egypt. E-mail: em.mohammed99@gmail.com

Received: 06-Aug-2019; **Revised:** 29-Aug-2019; **Accepted:** 30-Aug-2019; **Online first:** 14-Sep-2019

Funding: This research was partially funded by the National Research Centre, Egypt

Competing Interests: The authors have declared that no competing interests exist

Abstract

BACKGROUND: Human amniotic fluid-derived stem cells (hAF-MSCs) have a high proliferative capacity and osteogenic differentiation potential *in vitro*. The combination of hAF-MSCs with three-dimensional (3D) scaffold has a promising therapeutic potential in bone tissue engineering and regenerative medicine. Selection of an appropriate scaffold material has a crucial role in a cell supporting and osteoinductivity to induce new bone formation *in vivo*.

AIM: This study aimed to investigate and evaluate the osteogenic potential of the 2nd-trimester hAF-MSCs in combination with the 3D scaffold, 30% Nano-hydroxyapatite chitosan, as a therapeutic application for bone healing in the induced tibia defect in the rabbit.

SUBJECT AND METHODS: hAF-MSCs proliferation and culture expansion was done *in vitro,* and osteogenic differentiation characterisation was performed by Alizarin Red staining after 14 & 28 days. Expression of the surface markers of hAF-MSCs was assessed using Flow Cytometer with the following fluorescein-labelled antibodies: CD34-PE, CD73-APC, CD90-FITC, and HLA-DR-FITC. Ten rabbits were used as an animal model with an induced defect in the tibia to evaluate the therapeutic potential of osteogenic differentiation of hAF-MSCs seeded on 3D scaffold, 30% Nano-hydroxyapatite chitosan. The osteogenic differentiated hAF-MSCs/scaffold composite system applied and fitted in the defect region and non-seeded scaffold was used as control. The histopathological investigation was performed at 2, 3, & 4 weeks post-transplantation and scanning electron microscope (SEM) was assessed at 2 & 4 weeks post-transplantation to evaluate the bone healing potential in the rabbit tibia defect.

RESULTS: Culture and expansion of 2nd-trimester hAF-MSCs presented high proliferative and osteogenic potential *in vitro*. Histopathological examination for the transplanted hAF-MSCs seeded on the 3D scaffold, 30% Nano-hydroxyapatite chitosan, demonstrated new bone formation in the defect site at 2 & 3 weeks post-transplantation as compared to the control (non-seeded scaffold). Interestingly, the scaffold accelerated the osteogenic differentiation of AF-MSCs and showed complete bone healing of the defect site as compared to the control (non-seeded scaffold) at 4 weeks post-transplantation. Furthermore, the SEM analysis confirmed these findings.

CONCLUSION: The combination of the 2nd-trimester hAF-MSCs and 3D scaffold, 30% Nano-hydroxyapatite chitosan, have a therapeutic perspective for large bone defect and could be used effectively in bone tissue engineering and regenerative medicine.

Introduction

Human amniotic fluid stem cells (hAF-MSCs) derived from the second trimester are of particular importance as a source of a multipotent fetal stem cell and characteristically as a rich source of fetal progenitor cells including osteoblasts. Successful differentiation into osteogenic stem cells *in vitro* proposes their crucial role in regenerative medicine and bone regeneration [1].

Amniotic mesenchymal stem cells (AF-MSCs) have been used in animal models as a pre-clinical application. AF-MSCs have been applied on critically sized femoral defects of nude rat in combination with biomaterial scaffold and showed bone formation in rat femoral defect [2].

In contrast to embryonic stem cells, undifferentiated AF-MSCs propagate widely without inducing tumour [3]. Unlike adult-derived stem cells, the AF-MSCs cell lines propagated up to 250 population doublings retained long telomeres and a normal chromosomal karyotype [3]. Human amniotic fluid-derived stem cells (hAF-MSCs) are extensively multipotent and have been induced to differentiate into cell types representing each embryonic germ layer, including cells of osteogenic, adipogenic, chondrogenic, myogenic, endothelial, neuronal, and hepatic lineages [3-6].

To preserve and retain the physiological function and microstructure of the defected bones, regenerative medicine was explored very extensively during the last decades. Novel treatment techniques include utilising of nanocomposite scaffolds and sophisticated carriers for the targeting and delivery of bioactive molecules, mesenchymal stem cells and/or growth factors, providing both the structural exactness and the biochemical information to cells when they are differentiated into a particular type of tissue [7].

Nano-hydroxyapatite (HA) is considered as the most inorganic mineral in human bone tissue, therefore, HA artificial conformable materials are largely employed in the curing of bone defects originated by traffic accidents, trauma and bone disease [8-10]. In the bone defects remediation, some problems are expected to take place, such as low rate bone healing. The slower healing rate is especially recognised for patients with metabolic bone disorders and local osteoporosis [11].

Despite the magnificent role done by HA, stile it poses some drawbacks when it is used alone such as mechanical failure in load-bearing sites. In addition to that, the well-known composition of natural bone is considered as a composite material. This composite is made of inorganic (HA) and organic (collagen of type (I)) materials. Therefore, many of studies discussed the concept of the incorporation of the inorganic materials within the biopolymer matrix to form a composite material mimicking the microstructure of the bone [9, 12, 13].

Accordingly, nanocomposite scaffolds consisting of biodegradable polymers and/or ceramics consolidate the beneficial peculiarities of both materials. The effective carrier scaffolds can maintain their microstructure, physicochemical and physicomechanical properties at the implantation site [14]**.** Chitosan (C) is considered as a suitable polysaccharide for the fabrication of 3D scaffolds due to its impressive properties, such as biodegradability, biocompatibility, non-toxicity and bio-functionality [15].

The pre-clinical application of combined Stem cell technology with 3D biodegradable and nanostructure scaffold is a new trend of therapy in tissue engineering and bone repair, which is going to be investigated, evaluated and applied in this study.

Human AF-MSCs have the advantage of being a versatile precursor cell with great expansion capability. However, few studies have reported research results related to Nano-hydroxyapatite/chitosan (HA/C) scaffolds combined with hAF-MSCs in both *in vitro* and *in vivo*. Therefore, the aim of this study was directed to investigate the effect of the combination of 2nd-trimester hAF-MSCs with chitosan polymer scaffold contain 30% of HA ($^{W}/_{W}$ %) in the treatment of bone defect assessment.

Subjects and Methods

Second-trimester amniotic fluid samples (collected between the 14th and 18th weeks of gestation) were obtained by amniocentesis from six women, three samples only (n = 3) were successfully isolated. The age range was between 24 to 36 years old. The Ethics Committee of the National Research Centre, Cairo, Egypt, approved the study protocol and all participants gave informed consent.

Isolation of Mesenchymal stem cells

Mesenchymal stem cells were isolated from the collected amniotic fluid was done by centrifugation and pelleting of cells [3]. Subsequently, the cells were cultured in alpha minimal essential medium (α-MEM; Gibco BRL, Life Technologies B.V., Breda, Netherlands) containing 20% fetal bovine serum (FBS; Gibco ERL), 1% glutamax (Invitrogen), 100 U/ml penicillin (Gibco ERL), and 100 U/ml streptomycin (Gibco ERL) and 4 ng/ml basic fibroblast growth factor (bFGF; Sigma) and incubated at 37°C under standard conditions with 5% CO_2.

Culture, expansion and proliferation of hAF-MSCs

These steps were maintained in regular proliferation media to reach about 80% confluence, and then cells were passage and reseed. Manual scraping technique using cell scraper (Corning incorporated, Costar, Mexico) and collection of the cells, followed by centrifugation and re-suspension in regular proliferation media then re-seeding of cells in culture plates. Human AF-MSCs proliferation was done at 70% confluence of the 3rd passage and were used for osteogenic differentiation by exchanging the culture media into Dulbecco's Modified Eagle's Medium (DMEM) containing 20% FBS, 50 mmol/l L-

ascorbic acid 2-phosphate,10 mmol/l β-glycerol phosphate and 0.1 mmol/l dexamethasone as well as 100 µg/ml penicillin/ streptomycin and 1% glutamax [16]. A comparable control culture (MSCs in proliferation media) was made for each sample. Two similar sets that differ in incubation time were simultaneously generated; one set (plates in differentiation media and control plates) was maintained in corresponding culture media for 14 days before passed into characterisation protocols. The second set; same kind of plates retained in its culture media for 29 days before characterisation.

Osteogenic differentiation characterisation

This step was done using Alizarin Red staining for the detection of mineralised nodules developed in the differentiated cultures. In briefly, plates were washed three times with PBS and fixed in 70% ethanol at room temperature for an hour, washed with dH_2O before adding 2% Alizarin Red (pH 4.2). The plates were incubated at 37ºC for an hour with gentle shaking. Plates were washed with dH_2O until the dye's colour disappears. Carefully aspirate dH_2O, wash the plates with PBS and add enough dH_2O to cover the cellular monolayer to be ready for image capture by inverted microscope [17].

Expression of the surface markers in AF-MSCs

At the third passage (P3), AF-MSCs were assessed using Flow Cytometer, fluorescein-activated cell sorting (FACS) Calibur (BD Biosciences, USA). Cells were trypsinised (0.25% trypsin and 0.01% EDTA; w/v), washed twice with PBS supplemented with 0.5% Bovine Serum Albumin (BSA; Sigma-Aldrich, Saint Louis, MO, USA), and resuspended in PBS at a concentration of 2×10^5cells/20µl. Subsequently, the labelled cells were incubated with 10µl of the following fluorescein-labelled antibodies, CD34-PE, CD73-APC, CD90-FITC, and HLA-DR-FITC (BD Biosciences, USA) in dark place for 30 min at room temperature. Isotype-matched controls were performed for every analysis for the evaluation of possible nonspecific staining and autofluorescence [18].

Flow cytometry analysis operation started, and then a single colour immunofluorescence protocol was defined. A gate was set to include the population of interest, followed by running samples and 10.000 events were collected. Data analysis was executed to determine percentage positivity for the antibody [18]. Detailed immunophenotype analysis was carried out by flow cytometry using relevant markers. The cultured AF-MSCs express on their surface HLA-DR, CD 34, CD73, and CD90 and the percentages of positivity were calculated.

Osteogenic differentiation of AF-MSCs

Osteogenic differentiation of AF-MSCs performed on the 3D scaffold of 10 mm diameters and 3 mm heights *in vitro*. 3D Scaffold was used as a carrier for AF-MSCs, placed in 6-well culture plates, washed 3 times with 70 % ethanol, exposure to U.V for an hour and then washed twice with osteogenic medium (an hour for each rinse). AF-MSCs were seeded on the 3D scaffold at a density of $10x10^6$ and incubated at 37°C in osteogenic differentiation medium, DMEM containing 20% FBS, 100 µg/ml penicillin & streptomycin and 1% glutamax, L-ascorbic acid 2-phosphate, β-glycerol phosphate and dexamethasone for two and three weeks [16]. The scaffold carrying osteogenic differentiated AF-MSCs cells was fixed at 21st day using Glutaraldehyde and analysis by scanning electron microscope (SEM) [19].

In vivo study

The *in vivo* study, transplantation of human amniotic fluid stem cells (hAF-MSC) at the third passage (P3) was seeded on the 3D scaffold, 30% Nano-hydroxyapatite chitosan, and osteogenically differentiated for 3 weeks in osteogenic media and then applied to the induced tibia defect in the rabbit.

Ethics Approval

Ethical approval for this study was obtained from the National Research Centre Ethics Committee (approval number/16/263).

Animals and experiment design

A total of ten, six-month-old New Zealand White rabbits (1.5 – 2 Kg) were used for this study. Rabbits were classified into 3 groups as follows; G1: included 4 rabbits and were sacrificed at 2 weeks post-transplantation, G2: included 2 rabbits and were sacrificed at 3 weeks post-transplantation, and G3: included 4 rabbits and were sacrificed at 4 weeks of post-transplantation (Table 1). The defect has been transplanted with osteogenic differentiated hAF-MSCs progenitors cells seeded on the 3D scaffold *in vitro* (considered as an experimental target), and the tibia defect received 3D scaffold without osteogenic differentiated hAF-MSCs cells (considered as the control).

Table 1: Animal Groups Classification

Groups	G1	G2	G3
Rabbits no.	4	2	4
Sacrificed/Post-operation	2 weeks	3 weeks	4 weeks

Preoperatively, each rabbit has fasted for 12 hours. General anaesthesia was induced by intramuscular injection of ketamine hydrochloride (35 mg/kg BW) and xylazine (5 mg/kg BW) and

maintained throughout the surgical procedure.

The external incision in the tibia, the skin incisions (approximately 1.5 cm) were carried out (initiated) and extending to the muscles layers deep to the bone level, producing a defect cavity in the tibia 0.5 mm in diameter and 0.5 mm in depth. The cavities were prepared using standard round bur in a contra-angle handpiece running at approximately 10,000 rpm and abundantly irrigated with saline solution. Finally, the flaps were repositioned carefully and sutured in layers. Postoperative pain was managed by injection of buprenorphine (50 µg/kg BW) at every 2 hours for the first day. This experiment was conducted following the national and European guidelines for animal experiments.

The hAF-MSCs (approximately 2 million cells) at the third passage (P3) were seeded on the 3D scaffold, 30% Nano-hydroxyapatite chitosan, for two days in regular proliferation media and then replaced by osteogenic differentiation media after PBS washing, and incubated for 3 weeks at 37 ºC. Scanning electron microscope (SEM) was assessed to evaluate the osteogenic differentiation potential of hAF-MSCs osteogenic differentiated cells seeded on the 3D scaffold, 30% Nano-hydroxyapatite chitosan, *in vitro.* Meanwhile, osteogenic differentiated hAF-MSCs cells seeded on the 3D scaffold, 30% Nano-hydroxyapatite chitosan, was applied and fitted in the defect area of rabbit tibia to evaluate the new bone formation and bone healing impact.

Histological examination

Bone samples were fixed in 10% buffered formalin. Samples were decalcified in 0.5 M EDTA, pH 8.3 (Sigma-Aldrich, St. Louis, MO, USA). Parietal bones were then rinsed in PBS, dehydrated with graded ethanol, and embedded in paraffin. Transversal serial sections 5-6 µm thick were deparaffinized in xylene, hydrated with a series of graded ethanol, stained with hematoxylin/eosin (H&E), and examined under the optical microscope (CX41, Olympus, Tokyo, Japan) [20].

Preparation of Nano-hydroxyapatite

Artificial HA was prepared in the laboratory using the sol-gel method with an atomic ratio of Ca/P = (1.67) and pH = (10). Firstly, dissolving of 37.8 gm of calcium nitrate tetrahydrate in 1000 ml bi-distilled water. Meanwhile, 12.66 gm of diammonium hydrogen orthophosphate were also dissolved in another 1000 ml bi-distilled water containing polyethylene glycol as a dispersant agent. The required amounts of both stock solutions to give the desired Ca/P atomic ratio of 1.67 were mixed in room temperature, and the pH of the resulted mixture was adjusted to about 10 by the addition of a dilute NH_4OH solution with proper strength. The above stapes were followed by ageing and vigorous stirring of the obtained solution at its boiling point for about 2 h in a sealed container. The HA was collected from the solution by filtration and was washed three times with bi-distilled water, followed by drying at 100^{o}C overnight. A calcination temperature above 800^{o}C was applied to the dried powder to eliminate the other impurities such as nitrates and ammonia. The particle size and the morphology of the prepared HA were determined using TEM.

Preparation of scaffold Nano-composites

Acetic acid was used as the solvent to prepare the polymer solutions. By using 2 v % acetic acid solution, chitosan was dissolved using magnetic stirrer for 3 h, and the polymer solution was left overnight at room temperature to remove the air bubbles trapped in the viscous solution. Afterwards, 30% of hydroxyapatite was dispersed in bi-distilled water by 30 min ultrasonic treatment. The dispersed HA powders were mixed with the chitosan solution under agitation. The homogeneously mixed solution was poured in a syringe which was used as cylindrical moulds and immediately taken to deep freeze at –20^{o}C. After 24 h freezing the samples were quickly lyophilised for 36 hours. Finally, the scaffolds were cut into discs and analysed by XRD, and SEM-EDX measurements before *in vitro* and *in vivo* studies.

Transmission Electron Microscope

The morphology and particle size of the prepared hydroxyapatite was analysed using transmission electron microscope-TEM (JEM2010, Japan) working at 200 kv. Practically, 10 mg of HA powder was dispersed ethanol using the ultrasonic bath, and few drops of prepared suspension were dropped on the Cu grid. Afterwards, the grid was left to dry at room temperature and was further investigated by the TEM.

X-ray diffraction analysis (XRD)

X-ray diffraction analysis (XRD) was used to identify the phase of the prepared samples. The data was collected from a (Diano corporation made in the USA) diffractometer using monochromatic CuK_{α} radiation (λ=1.5406**Å**) with scanning rate 0.1^{o} in the 2θ ranging from 10 to 80^{o} step radiation. Voltage and current were set at 40 kV and 40 mA, respectively.

Scanning Electron Microscope

The scaffold microstructure was studied using JSM 6360 LV SEM (JEOL, Japan). In detail, the cross-sectional view for the prepared scaffold was studied through mounting the internal scaffold structure on metal stubs and was coated with gold

before being examined. Additionally, X-ray elemental analysis (EDAX) was carried out for the samples pre-*in vitro* and *in vivo* studies to assess the presence of the inorganic elements within the examined scaffold.

Moreover, SEM images were recorded for the scaffold with and without hAF-MSCs osteogenic differentiated cells *in vitro* and *in vivo* to evaluate the effect of the combination of hAF-MSCs osteogenic differentiated cells and scaffold on bone healing rate. Practically, *in vitro* SEM images were obtained upon seeding of hAF-MSCs on the scaffold surface in 12 well plates for 21 days in the osteogenic media. In details, the scaffolds were washed 3 times with 70 % ethanol, exposed to U.V light for 2 h, and then washed twice with the culture medium.

Results

Proliferation and culture expansion of hAF-MSCs

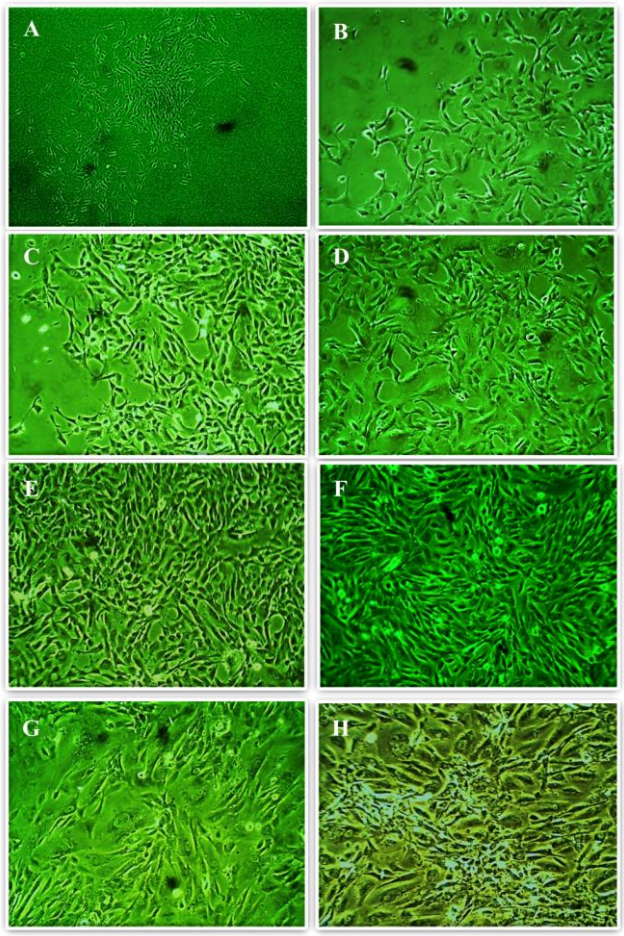

Figure 1: Proliferation and culture expansion of hAF- MSCs at different passage. (A & B) P0 at 7 & 21 days respectively; (C&D) P1 at 7 &17 days respectively; (E&F) P2 at 7 &19 days respectively; (G&H) P3 at 7 & 21 days respectively, magnification X10

Human AF-MSCs was cultured and expanded in regular proliferation media. Colonies of hAF-MSCs appeared in the primary culture (P0) after 7-10 days from the initial cell plating day. Cells aggregated from central to peripheral side of the plate till reaching 75% confluence by the end of this passage (Figs. 1A, B respectively). At the beginning of the first passage (P1), hAF-MSCs displayed typical fibroblast-like cells morphology and presented a higher proliferation rate by the end of this passage (Figs. 1C, D respectively). Human AF-MSCs presented typical mesenchymal cell morphology in the subsequent passages and experienced further proliferation and expansion in the second passage (P2) (Figs. 1E, F) and third passage (P3) (Figs. 1G, H).

Osteogenic differentiated AF-MSCs on 14th and 28th days

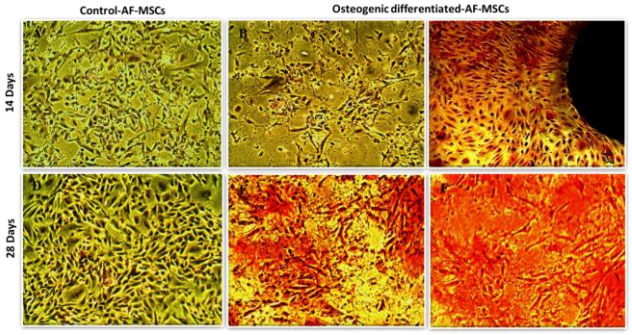

Figure 2: Alizarin red staining of osteogenic differentiated AF-MSCs on 14 and 28 days, A) Control at 14 days of culture showed no red staining; B) Osteogenic differentiated AF-MSCs cells at 14 days showed few stain spots in centre of the plate; C) moderate red staining patches were detected in peripheral side of the plate; D) Control at 28 days of culture showed very weak red staining spots; E) Strong red staining patches of osteogenic differentiated AF-MSCs at 28 days in the central of the plate; F) Stronger red staining intensity of osteogenic differentiated AF-MSCs cells in peripheral side of the plate

Osteogenic differentiation of hAF-MSCs seeded on Scaffold after three weeks in vitro

The hAF-MSCs cells were seeded and osteogenically differentiated on the 3D scaffold, Nano-hydroxyapatite chitosan, in the osteogenic media for 3 weeks *in vitro,* small to large black areas represented scaffold filled with AF-MSCs osteogenic differentiated and calcium deposits all over the plate were observed using an inverted microscope (Figs. 3A & B). Moreover, this finding was confirmed by using the electron microscope scanned (EMS) indicating the osteogenic differentiated hAF-MSCs was penetrated the pore and filled with calcium nodule deposits which will be ready for animal transplantation, bone repair, and regeneration (Fig. 3D) compared to the non-seeded scaffold (Fig. 3C).

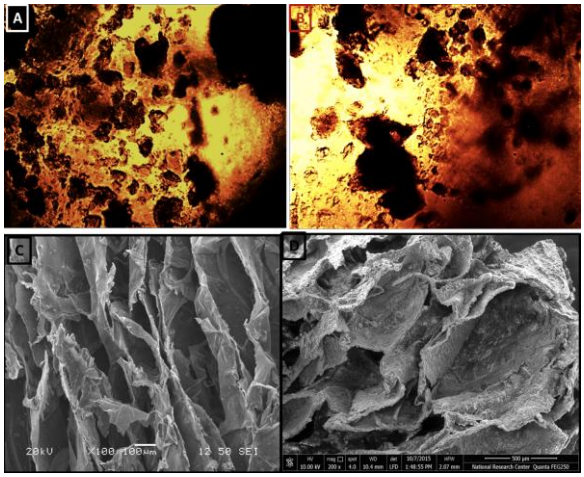

Figure 3: Osteogenic differentiation of hAF-MSCs seeded on Scaffold after 3 weeks in vitro. (A) & (B) Osteogenic differentiated of hAF-MSCs seeded on scaffold represented by inverted microscope images. (C) Non-seeded Scaffold (SEM, Scale Bar: 100 µm); (D) hAF-MSCs osteogenic differentiated seeded on the scaffold (SEM, Scale Bar: 500 µm)

Flow cytometric analysis

Flow cytometric analysis was performed to detect the AF-MSCs immunophenotypes.

Table 2: Flow-cytometry parameters in hAF-MSCs

hAF-MSCs Surface marker	Positivity rate
CD73	42.1%
CD90	2.4%
CD34	0.2%
HLA-DR	0.1%

The percentage were positive for both CD73 and CD90 cell surface markers showed 42.1 % and 2.4% respectively, while were negative for both CD34 and HLA-DR cell surface markers showed 0.2%, and 0.1% respectively (Table 2) (Fig. 4).

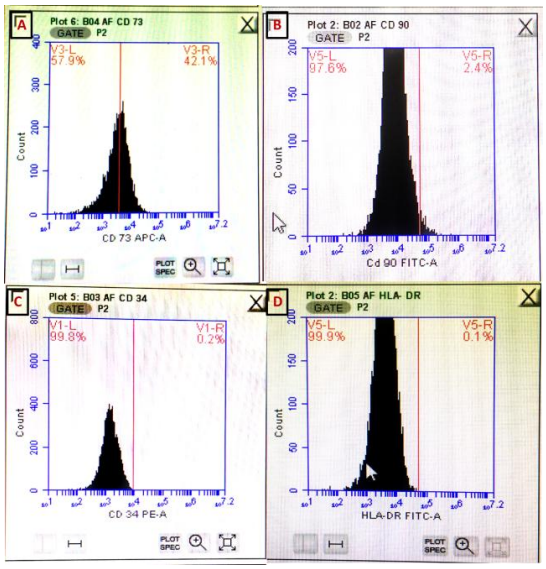

Figure 4: Flow cytometric analysis for hAF-MSCs. (A) & (B) hAF-MSCs were positive for both CD73 and CD90 cell surface markers 42.1% & 2.4% respectively. (C) & (D) hAF-MSCs were negative for both CD34 and HLA-DR cell surface markers 0.2% & 0.1% respectively

Histological results

At two weeks post-transplantation, histological examination of sections transplanted with osteogenic differentiated hAF-MSCs cells seeded on the 3D scaffold, 30% Nano-hydroxyapatite chitosan, showed large areas of newly formed bone that were observed directly nearby to the host bone as compared to the control (Fig. 5A). In contrast, the control (non-seeded scaffold) showed areas filled with structurally and morphologically rearranged fibrous tissue consistent with the failure to repair the bone defect (Fig. 5B).

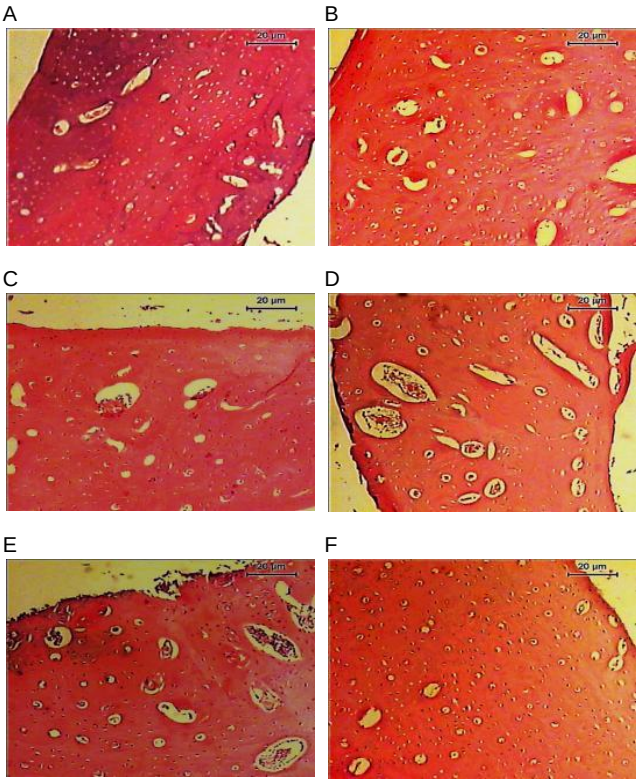

Figure 5: Histopathological Sections of rabbits transplanted by hAF-MSCs and Scaffold. A): Osteogenic differentiated hAF-MSCs seeded on the 3D scaffold, 30% Nano-hydroxyapatite chitosan after 2 weeks showing large areas of new bone formation visible immediately nearby to the host bone compared with the control (non-seeded scaffold). Notice the occurrence of an infinite network of vessels is obviously in the not yet mineralized construct area, B) Control, after 2 weeks showing areas filled with structurally and morphologically prearranged fibrous tissue consistent with failure to repair the bone defect; C) hAF-MSCs/scaffold, after three weeks shows large areas of mature formed in the defect. Few vacuoles filled with collagen were noticed D) Control after 3 weeks shows limited bone regeneration and large bone defect remaining. Notice that the defect is filled primarily with connective tissues; E) hAF-MSCs/scaffold after 4 weeks show large mature bone mostly filed the whole defect. Few vacuoles filled with collagen were noticed; F) Control after 4 weeks shows limited bone regeneration and large bone defect remaining. Notice that the defect is filled primarily with connective tissues (H&E stain; Scale bar: 20 µm)

At three weeks post-transplantation, sections of bone defect transplanted with osteogenic differentiated hAF-MSCs/scaffold showed large areas of mature formed bone in the defect site. Few vacuoles filled with collagen were noticed as compared to control one (Fig. 5C). However, the

control (non-seeded scaffold) showed limited bone regeneration with a large bone defect area remaining. The defect was filled primarily with connective tissues (Fig. 5D).

At four weeks post-transplantation, histological examination of bone **s**ections defect transplanted with osteogenic differentiated hAF-MSCs/scaffold showed mature bone formation mostly filled the whole defect area. Few vacuoles filled with collagen were noticed (Fig. 5E). However, the control (non-seeded scaffold) showed limited bone regeneration and large bone defect area remaining. Notice that the defects were filled mainly with connective tissues (Fig. 5F).

Morphology of the prepared Nano-hydroxyapatite

The morphology and the size of the prepared Nano-hydroxyapatite were evaluated by TEM as represented in Fig. 6. The Nano-hydroxyapatite particles are presented in the nanoscale with a range of 20-30 nm. Semisphere morphology was observed for aggregated particles of hydroxyapatite.

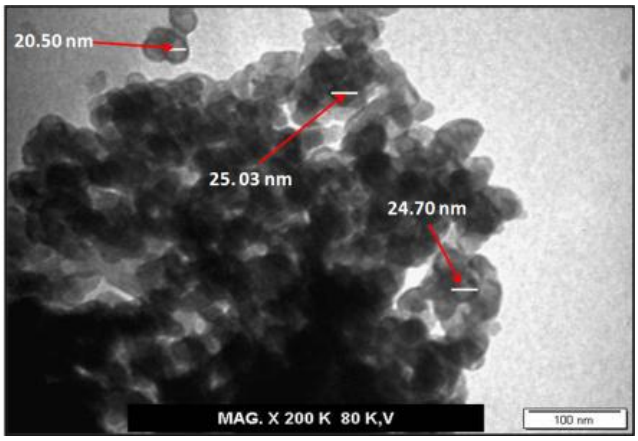

Figure 6: TEM image of the prepared Nano-hydroxyapatite (TEM, Scale Bar: 100 µm)

Scanning Electron Microscope results

The XRD technique is employed to assess the phase purity, the level of crystallinity and changes of the prepared nanocomposites. XRD method is based on the coherent scattering of X-rays by an ordered lattice, in this case, a crystal in which the atoms are periodically ordered. Interference of the radiation with the crystal lattice leads to a distinct distribution of diffracted intensity as a function of the measuring angle 2θ.Fig.7a shows the X-ray diffraction pattern of the prepared hydroxyapatite (HA). Several peaks were observed at approximately 25.8°, 29.1, 30.6° and 31.8°C, these peaks are corresponding to the diffraction planes (211), (002), (210) and (300) of the hydroxyapatite (HA) crystallites, respectively, that confirms the formation hydroxyapatite as early reported [21, 22]. It is worthy noted that upon the formation of chitosan/hydroxyapatite composite scaffold, no remarkable changes were observed for the crystallisation of the HA particles. However, minor crystallisation decrease was noted (Fig.7b). In addition to that, the characteristic crystalline peaks of HA were significantly shifted, due to the expected interface binding that takes place between hydroxyapatite particles and chitosan matrix.

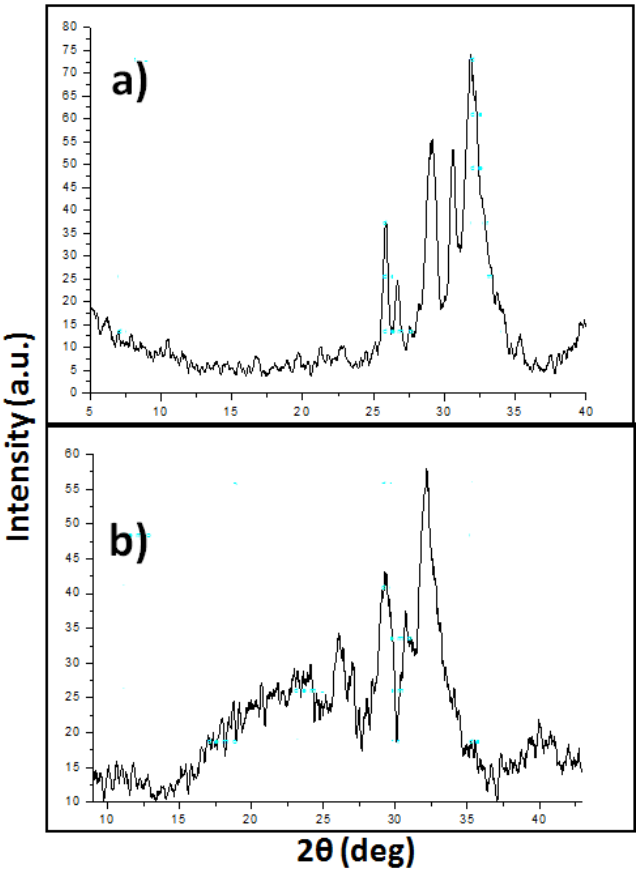

Figure 7: XRD analysis of a) the prepared Nano-hydroxyapatite and b) chitosan /hydroxyapatite composite scaffold

The scanning electron microscope (SEM-EDX) micrographs of the prepared scaffold composite (HC30) is shown in Fig. 8. The SEM images provide direct information about the mullet-porous structure of the as-prepared hydroxyapatite/chitosan scaffold nano-composite. SEM images demonstrated a large number of pores around the size of 200 µm–700 µm. These pores are connected to form an interconnected porous network. The rough surface that was observed for prepared composites was attributed to the incorporation of hydroxyapatite in the composite. The HA particles were embedded well in the chitosan matrix. From the EDX spectra of the prepared hydroxyapatite /chitosan scaffold nanocomposite (Fig. 8), illustrated the recorded elements within the investigated scaffold as following; Ca, P, C and O.

Furthermore, the cells attachment on the scaffold surface cultured in the osteogenic medium at culture time 21 days (Fig. 9a), was also investigated using SEM. “C” corresponds to cells, “J” is the cell-cell

junctions, “M” mineralisation is also detected. Extracellular matrix (EX), attached to scaffold surface, of chitosan /hydroxyapatite composite scaffold.

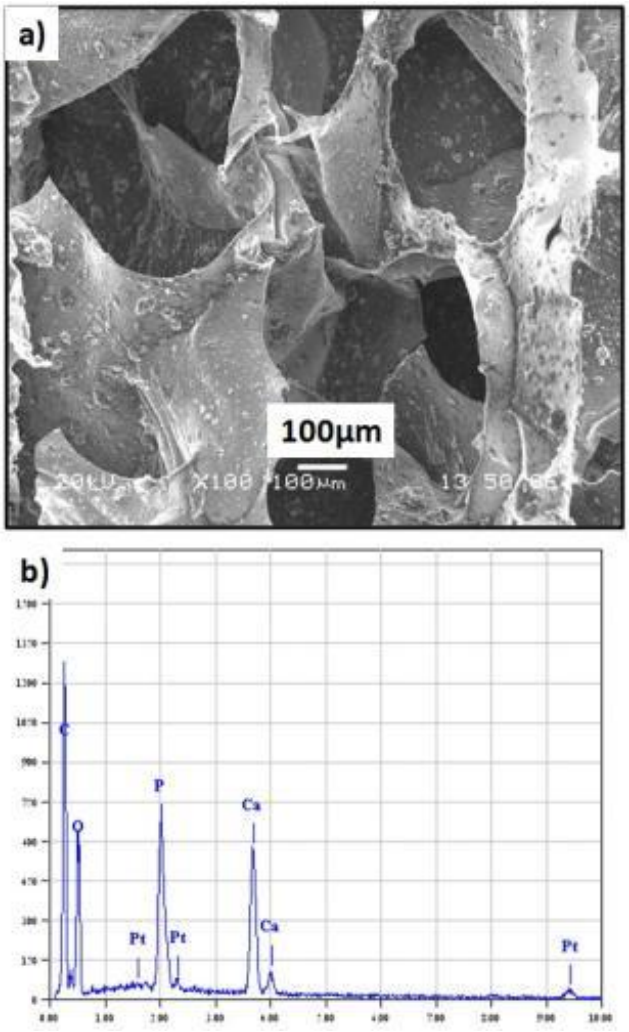

Figure 8: Illustration of a) SEM image for the microstructure (Scale Bar: 100 µm) and b) EDX elemental analysis for the chitosan /hydroxyapatite composite scaffold

In details, it is very clear that human amniotic fluid-derived stem cells (hAF-MSCs)are grown on scaffold surface and have displayed an elongated shape and spread out discretely within the pores and on the surface of the scaffold.

Also, mineral aggregates formation was noted after 21 days of culture, thus denoting the osteogenic activity of prepared scaffold. The higher magnification image (Fig.9b) that show the surface of the cells on prepared scaffolds appeared to be smoother than that on the scaffolds, indicating greater extracellular matrix (EX) depositions and fibrous networks on scaffolds surface as well as attached cells.

In addition to that, the *in vivo* bone healing was investigated by using SEM (Fig.10). Post-transplantation of the prepared scaffold was transplanted into the rabbit's tibia defect, revealed normal healing of the bone tissues with no abnormalities over the site of the operation.

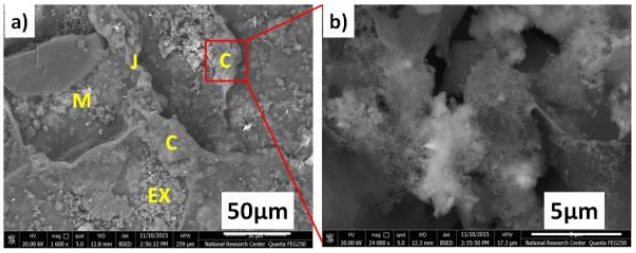

Figure 9: SEM images of a) chitosan/hydroxyapatite composite scaffold and b) Zoom in mineralisation on the scaffold surface (SEM, Scale Bar: 50 and 5 µm, respectively)

All rabbits were healthy and did not present signs of oedema during the post-transplantation period. The scaffolds were in direct contact with new bone without any fibrous encapsulation and almost completely covered with new bone (NB) indicating that scaffolds were highly bioactive as well as biocompatible.

Few remains of scaffolds were still found in the defect, as well as unfilled margins (Figs.10a &10c). They were in direct contact with new bone without any fibrous encapsulation and almost completely covered with bone indicating that scaffolds were highly bioactive as well as biocompatible. The induced bone defect in the rabbit tibia transplanted with the non-seeded scaffold at two and four weeks post-transplantation was semi-healed with highly mineralised bone matrix, and the defect holes remain semi-opened (Figs. 10a & 10c).

For the defect transplanted with osteogenic differentiated hAF-MSCs/scaffold at 2 weeks post-transplantation (Fig. 10b), new bone formation progressed from the deep end walls of the defect regions in-wards. Complete bone integration was detected for the transplanted osteogenic differentiated hAF-MSCs/scaffold at 4 weeks post-transplantation (Fig.10d).

The new bone was formed in continuity with the transplant surface from the cortical bone at the defect site into the marrow space. Also, the results of SEM made for the non-seeded scaffolds transplanted *in vivo* revealed that the bioactive degradable scaffolds have a great response with the host bone and the remodelling proceeded at the scaffolds-bone interface. The induced bone defects in the rabbit tibia at 4 weeks post-transplantation were completely closed by mineralised (M) bone matrix, collagen fibres (CF) and differentiated cells (DC) (Fig. 10 d). There was evidence of new bone formation on the surface of all implants with no evidence of fibrous encapsulation.

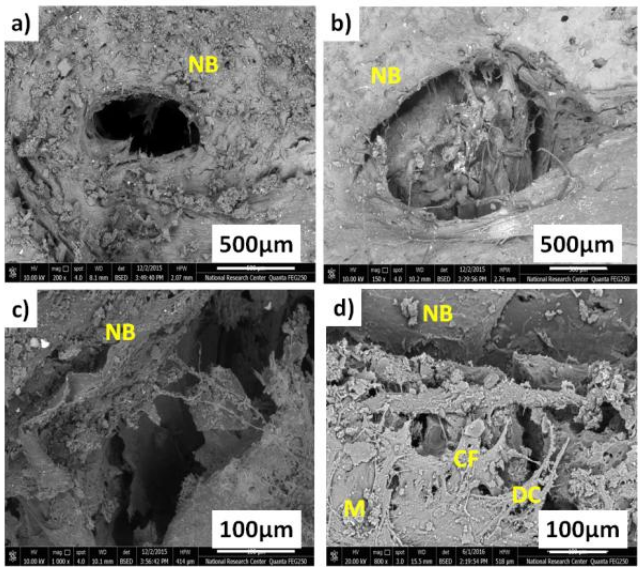

Figure 10: SEM images of chitosan/hydroxyapatite composite scaffold after in vivo implantation. a) control, non-seeded Scaffold after 2 weeks, b) osteogenic differentiated hAF-MSCs cells seeded on Scaffold after 2 weeks, c) control, non-seeded Scaffold after 4 weeks and d) osteogenic differentiated hAF-MSCs cells seeded on Scaffold after 4 weeks (SEM, Scale Bar: 100 µm)

Discussion

Human amniotic stem cell (hAF-MSCs) has a high proliferative capacity and osteogenic differentiation potential *in vitro* provides a very promising source for bone repair applications. Moreover, the combination of hAF-MSCs and three-dimensional (3D) scaffold is considered to be a promising approach for therapeutic purpose applications in bone tissue engineering and regenerative medicine.

In our previous study, results revealed the 2nd-trimester hAF-MSCs used in repairing the induced spinal cord defect in rat model had the priority of bone healing efficiency compared to both the 3rd-trimester hAF-MSCs and hBM-MSCs transplanted into the same animal model [23]. Accordingly, we suggested that the 2nd-trimester hAF-MSCs cells may represent a valuable healing prospect in combination with 3D scaffolds for bone regeneration in the rabbit tibia defect.

The assessment of the combination of the 2nd-trimester hAF-MSCs with the 3D scaffold, 30% Nano-hydroxyapatite chitosan, in our study demonstrated the osteogenic induction for three weeks *in vitro;* cells penetrated the scaffold porous, filled with calcium deposited and were ready for repairing the bone defect in a rabbit model. This finding is consistence with Maraldi et al., who conducted his study on a rat model. They support the idea of the efficiency of scaffold material, fibroin, combined with AF-MSCs in healing critical-size bone defects [24]. Our hAF-MSCs subjected an osteogenic differentiation *in vitro* for 21 days on the 3D scaffold, 30% Nano-hydroxyapatite chitosan, showed great mineralisation and repairing potential for the induced bone defect in the rabbit. Interestingly, Peister et al. demonstrated that AF-MSCs have the effect to differentiate for 28 days on 3D medical-grade poly-e-caprolactone (mPCL) scaffolds *in vitro* producing seven times more mineralised matrix when transplanted subcutaneously in the rat model. Findings of this study suggest that AF-MSCs could be an effective cell source for efficient repair of large bone defects [25].

However, our *in vivo* study revealed the combination of osteogenic differentiated hAF-MSCs cells and scaffold enhanced the bone healing efficiency in the bone defect of rabbit at 4 weeks post-transplantation comparing to the control (non-seeded scaffolds). Roccio et al., in 2012, carried out a comparative assessment of fibroin scaffolds combined with human dental pulp stem cells (hDP-MSCs) and amniotic fluid stem cells (hAF-MSCs) for repairing the cranial bone defects in immunocompromised rats [26]. They reported a significant efficient healing property of the combination of stem cells/fibroin bioengineered scaffold in repairing large animal cranial defects. This finding could be a starting point for human large bone defects regeneration in craniofacial surgery [26]. Moreover, Kim et al., have already noted an inconsistency with Roccio`s results that hAF-MSCs seeded on another type of 3D scaffold, collagen matrix extracted from porcine bladder submucosa matrix (BSM) and poly (lactide-co-glycolide) (PLGA), offered an appropriate microenvironment that enhanced osteogenic differentiation of hAF-MSCs *in vitro* and could be used in bone tissue engineering [27].

In the present study, AF-MSCs were examined for surface and differentiation markers percentages on cells using flow cytometer as an indication of Mesenchymal stem cells (MSC). Flow cytometric assays were performed within the tested cell population for CD34, CD90, and CD73 in addition to HLA-DR. Isolated AF-MSCs cells in this study revealed moderate expression of CD73 (42.1%) in addition to the negativity of CD34 and HLA-DR (0.2% and 0.1 %respectively) and weak expression of CD90 (2.4%). Regarding CD34, our results came by De Rosa et al., and Fei et al., studied the phenotypic characterisation of AF-MSCs [28, 29]. By flow cytometric assays; found them negative for CD34. Moreover, our results also agreed with Zhou et al., stated that AF-MSC must express CD105, CD73 and CD90 and lack the expression of CD45, CD34, CD14, CD11b, CD79a, CD19 and HLA-DR surface molecules. In the same context, in this study, CD73 was positively expressed (42.1%); while CD34 and HLA-DR were negatively expressed (0.2% and 0.1% respectively); results of which had the same opinion

as Markmee et al., found CD73 (49.85%), CD34 (0.3%) and HLA DR (0%) [30].

Nevertheless, Spitzhorn et al. found that AF-MSCs obtained during C-sections showed the typical MSC cell surface marker expression of CD73, CD90, and CD105 by the parallel absence of the hematopoietic markers CD14, CD20 and CD34 [31]. The analysis of the isolated cells in Fei et al., study, revealed negative expression of the hematopoietic stem cell marker, CD34 and some cells were weakly positive for MHC Class II antigens (HLA-DR and HLA-DQ) [29], which agree with the results found in the present study.

Additionally, regarding, HLA-DR testing, cells were found negative as the previous results of Zhou et al., [32]. However, our study didn't reveal strong positivity for CD90, unlike Zhou et al., Savickiene et al., and Markmee et al. [30], [32], [33]. On the contrary, Fei et al. found isolated cells in his study not expressing markers of hemopoietic lineage such as CD105 (SH2), CD70 (SH3/4), CD29, CD16, CD44, and CD90 [29].

The analysis of our histopathological results revealed a distinctive increase in bone regeneration in the tibia defect of a rabbit when received the osteogenic differentiated hAF-MSCs cells/scaffold composite system which mostly filled with mature bone and few vacuoles filled with collagen at 4 weeks post-transplantation. However, the control (non-seeded scaffold) presented fewer, smaller mineralised tissue, limited new bone formation, and there was a large bone defect area still not filled with bone. These findings identified the highest bone healing efficiency with complete healing of the bone defect at 4 weeks post-transplantation. However, the least bone healing potential was observed at 2 weeks post-transplantation; these findings were consistency with the Scanning electron microscope (SEM) results. There is a satisfactory agreement between our results and those of Rodrigues et al., despite the difference in scaffold type, transplantation time, an animal model [34].

It is well known that hydroxyapatite mineral forms about 70 wt. % of natural bone. Collagen and water represent the remaining portion (20-30) wt. %. Nano-structured hydroxyapatite crystals are aligned along the collagen fibres within the water phase [35]. Herein, the prepared hydroxyapatite possessed similar morphology and particle size for those of the natural bone. The XRD results for the prepared scaffolds revealed that incorporation of the Nano-hydroxyapatite didn't alert the physical stability and crystalline nature of obtained scaffold. The low crystallinity of the obtained HA that was much similar to the apatite in natural bone could improve the biodegradability (Fig. 7). It is well known that bone biological characterises of scaffolds are affected by their chemical composition, crystallinity, crystal orientation and porous structures [36].

SEM images revealed the scaffolds would allow the attachment and spreading of the cells while keeping a normal cellular morphology as confirmed with recorded pore sizes (200 µm – 700 µm). These pores are associated with each other to form an interconnected porous network. This network directly facilitated the normal activity of the cells such as nutrition transport, ions exchange and elimination of the cells biological leftover. Porous structure enables the cells infiltration within the pore cavities and provides enough nutrition and blood supply through penetration and circulation [37], [38].

It is worth to highlight that the choice of scaffold depends on the specific tissue to be engineered. It is generally recognised that the chemical properties of materials can influence the cellular behaviour of osteoblasts [12], [39]. SEM images for the current investigated scaffold suggested that the 30 CH scaffold of higher support osteogenic activity and these results were in the same line with early reported studies [12], [39].

Chitosan-nanocomposite scaffolds, the biomaterials that were utilised in the current research, are deemed osteoconductive materials to both cell adhering and tissue ingrowth, and it couples biomaterial resorption with bone formation [40], [41]. However, The SEM images of hAF-MSCs seeded on the 3D scaffold, 30% Nano-hydroxyapatite chitosan, have demonstrated a higher healing potential compared to the control, non-seeded scaffold, 30% Nano-hydroxyapatite chitosan at 2 and 4 weeks post-transplantation.

Our investigations into this area are still ongoing, and further investigations on studying different stem cell sources as well as various scaffold materials will advance our knowledge about the contribution of stem cells progenitor and scaffold composite system to the field of bone tissue engineering.

In conclusion, based on our *in vitro* and *in vivo* findings, we suggest that the 2nd-trimester hAF-MSCs in combination with the 3D scaffold, 30% Nano-hydroxyapatite chitosan, could significantly promote and enhance the bone healing efficiency in the rabbit model. Furthermore, this approach can be used as an outstanding system for functional bone treatment for the repair of large bone defect in human, bone tissue engineering and regenerative medicine.

Acknowledgements

All authors acknowledge the National Research Centre for funding this project. We thank the participant for providing their samples.

References

1. Cananzi M, Atala A, De Coppi P. Stem cells derived from amniotic fluid: new potentials in regenerative medicine. Reprod Biomed Online. 2009; 18(Suppl 1):17-27. https://doi.org/10.1016/S1472-6483(10)60111-3

2. Dupont KM, Sharma K, Stevens HY, Boerckel JD, Garcia AJ, Guldberg RE. Human stem cell delivery for treatment of large segmental bone defects. Proc Natl Acad Sci U S A. 2010; 107(8):3305-3310. https://doi.org/10.1073/pnas.0905444107 PMid:20133731 PMCid:PMC2840521

3. De Coppi P, Bartsch G, Jr., Siddiqui MM, Xu T, Santos CC, Perin L, Mostoslavsky G, Serre AC, Snyder EY, Yoo JJ et al. Isolation of amniotic stem cell lines with potential for therapy. Nat Biotechnol. 2007; 25(1):100-106. https://doi.org/10.1038/nbt1274 PMid:17206138

4. De Coppi P, Callegari A, Chiavegato A, Gasparotto L, Piccoli M, Taiani J, Pozzobon M, Boldrin L, Okabe M, Cozzi E et al. Amniotic fluid and bone marrow derived mesenchymal stem cells can be converted to smooth muscle cells in the cryo-injured rat bladder and prevent compensatory hypertrophy of surviving smooth muscle cells. J Urol. 2007; 177(1):369-376. https://doi.org/10.1016/j.juro.2006.09.103 PMid:17162093

5. Delo DM, De Coppi P, Bartsch G, Jr., Atala A. Amniotic fluid and placental stem cells. Methods Enzymol. 2006; 419:426-438. https://doi.org/10.1016/S0076-6879(06)19017-5

6. Kolambkar YM, Peister A, Soker S, Atala A, Guldberg RE. Chondrogenic differentiation of amniotic fluid-derived stem cells. J Mol Histol. 2007; 38(5):405-413. https://doi.org/10.1007/s10735-007-9118-1 PMid:17668282

7. Caramella C, Conti B, ModenaT, Ferrari F, Bonferoni M C, Genta I, Rossi S, LuisaTorre M, Sandri G, Sorrenti M et al. Controlled delivery systems for tissue repair and regeneration. Journal of Drug Delivery Science and Technology. 2016; 32 206-228. https://doi.org/10.1016/j.jddst.2015.05.015

8. Shen S, Cai S, Li Y, Ling R, Zhang F, Xu G, F W. Microwave aqueous synthesis of hydroxyapatite bilayer coating on magnesium alloy for orthopedic application. Chemical Engineering Journal. 2017; 309:278-287. https://doi.org/10.1016/j.cej.2016.10.043

9. Roh HS, Lee CM, Hwang YH, Kook MS, Yang SW, Lee D, Kim BH. Addition of MgO nanoparticles and plasma surface treatment of three-dimensional printed polycaprolactone/hydroxyapatite scaffolds for improving bone regeneration. Mater Sci Eng C Mater Biol Appl. 2017; 74:525-535. https://doi.org/10.1016/j.msec.2016.12.054 PMid:28254327

10. Liu Y, Luo D, T. W. Hierarchical Structures of Bone and Bioinspired Bone Tissue Engineering. Small. 2016; 12(34):4611-4632. https://doi.org/10.1002/smll.201600626 PMid:27322951

11. Hunziker EB, Enggist L, Kuffer A, Buser D, Liu Y. Osseointegration: the slow delivery of BMP-2 enhances osteoinductivity. Bone. 2012; 51(1):98-106. https://doi.org/10.1016/j.bone.2012.04.004 PMid:22534475

12. Tohamy KM, Mabrouk M, Soliman IE, Beherei HH, Aboelnasr MA. Novel alginate/hydroxyethyl cellulose/hydroxyapatite composite scaffold for bone regeneration: In vitro cell viability and proliferation of human mesenchymal stem cells. Int J Biol Macromol. 2018; 112:448-460. https://doi.org/10.1016/j.ijbiomac.2018.01.181 PMid:29408578

13. Li H, Zhou C-R, Zhu M-Y, Tian J-H, Rong J-H. Preparation and Characterization of Homogeneous Hydroxyapatite/Chitosan Composite Scaffolds via In-Situ Hydration. Journal of Biomaterials and Nanobiotechnology. 2010; 1(1):42-49. https://doi.org/10.4236/jbnb.2010.11006

14. Meliegy E, Mabrouk M, Kamaln GM, Awad SM, El-Tohamy AM, El-Gohary MI. Anticancer drug carriers using dicalcium phosphate/dextran/CMCnanocomposite scaffolds. Journal of Drug Delivery Science and Technology. 2018; 45:315-322. https://doi.org/10.1016/j.jddst.2018.03.026

15. El-Meliegy E, Mabrouk MS, El-Sayed AM, Abd El-Hady BM, Shehata MR, Hosny WM. Novel Fe2O3-doped glass /chitosan scaffolds for bone tissue replacement. Ceramics International. 2018; 44(8):9140-9151. https://doi.org/10.1016/j.ceramint.2018.02.122

16. Zhang Q, Wang X, Chen Z, Liu G: Semi-quantitative RT-PCR analysis of LIM mineralization protein 1 and its associated molecules in cultured human dental pulp cells. Arch Oral Biol. 2007; 52(8):720-726. https://doi.org/10.1016/j.archoralbio.2007.02.005 PMid:17368558

17. Tsukamoto Y, Fukutani S, Shin-Ike T, Kubota T, Sato S, Suzuki Y, Mori M. Mineralized nodule formation by cultures of human dental pulp-derived fibroblasts. Arch Oral Biol. 1992; 37(12):1045-1055. https://doi.org/10.1016/0003-9969(92)90037-9

18. Jaroszeski RH. Flow Cytometry Protocols. Eds Humana Press, Totowa, 1998:217-238. https://doi.org/10.1385/0896033546

19. Zavatti M, Bertoni L, Maraldi T, Resca E, Beretti F, Guida M, Giovanni B, La Sala, Pol AD. Critical-size bone defect repair using amniotic fluid stem cell/collagen constructs: Effect of oral ferutinin treatment in rats. Life Sci. 2015; 121(15):174-183. https://doi.org/10.1016/j.lfs.2014.10.020 PMid:25445219

20. Carleton HM, Drury RAB, Wallington EA. Carleton's Histological Technique. Oxford Medical Publications, 1980.

21. Murugan R, Rao KP, Kumar TSS. Heat-deproteinated xenogeneic bone from slaughterhouse waste: physico-chemical properties. Bulletin of Materials Science. 2003; 26(5):523-528. https://doi.org/10.1007/BF02707351

22. Nikpour MR, Rabiee SM, JahanshahiM. Synthesis and characterization of hydroxyapatite/chitosan nanocomposite materials for medical engineering applications. Composites. 2012; Part B, 43:1881-1886. https://doi.org/10.1016/j.compositesb.2012.01.056

23. Mohammed EEA, El-Zawahry M, Farrag ARH, Aziz NNA, Sharaf-ElDin W, Abu-Shahba N, Mahmoud M, Gaber K, Ismail T, Mossaad MM et al. Osteogenic Differentiation Potential of Human Bone Marrow and Amniotic Fluid-Derived Mesenchymal Stem Cells in Vitro & in Vivo. Open Access Maced J Med Sci. 2019; 7(4):507-515. https://doi.org/10.3889/oamjms.2019.124 PMid:30894903 PMCid:PMC6420942

24. Maraldi T, Riccio M, Resca E, Pisciotta A, La Sala GB, Ferrari A, Bruzzesi G, Motta A, Migliaresi C, Marzona L et al. Human amniotic fluid stem cells seeded in fibroin scaffold produce in vivo mineralized matrix. Tissue Eng Part A. 2011; 17(21-22):2833-2843. https://doi.org/10.1089/ten.tea.2011.0062 PMid:21864161

25. Peister A, Deutsch ER, Kolambkar Y, Hutmacher DW, Guldberg RE. Amniotic fluid stem cells produce robust mineral deposits on biodegradable scaffolds. Tissue Eng Part A. 2009; 15(10):3129-3138. https://doi.org/10.1089/ten.tea.2008.0536 PMid:19344289 PMCid:PMC2792053

26. Riccio M, Maraldi T, Pisciotta A, La Sala GB, Ferrari A, Bruzzesi G, Motta A, Migliaresi C, De Pol A. Fibroin scaffold repairs critical-size bone defects in vivo supported by human amniotic fluid and dental pulp stem cells. Tissue Eng Part A. 2012; 18(9-10):1006-1013. https://doi.org/10.1089/ten.tea.2011.0542 PMid:22166080

27. Kim J, Jeong SY, Ju YM, Yoo JJ, Smith TL, Khang G, Lee SJ, Atala A. In vitro osteogenic differentiation of human amniotic fluid-derived stem cells on a poly(lactide-co-glycolide) (PLGA)-bladder submucosa matrix (BSM) composite scaffold for bone tissue engineering. Biomed Mater. 2013; 8(1):014107. https://doi.org/10.1088/1748-6041/8/1/014107 PMid:23353783

28. De Rosa A, Tirino V, Paino F, Tartaglione A, Mitsiadis T, Feki A, d'Aquino R, Laino L, Colacurci N, Papaccio G. Amniotic fluid-derived mesenchymal stem cells lead to bone differentiation when cocultured with dental pulp stem cells. Tissue Eng Part A. 2011; 17(5-6):645-653. https://doi.org/10.1089/ten.tea.2010.0340 PMid:20919950

29. Fei X, Jiang S, Zhang S, Li Y, Ge J, He B, Goldstein S, Ruiz G. Isolation, culture, and identification of amniotic fluid-derived mesenchymal stem cells. Cell Biochem Biophys. 2013; 67(2):689-

694. https://doi.org/10.1007/s12013-013-9558-z PMid:23508888

30. Markmee R, Aungsuchawan S, Narakornsak S, Tancharoen W, Bumrungkit K, Pangchaidee N, Pothacharoen P, Puaninta C. Differentiation of mesenchymal stem cells from human amniotic fluid to cardiomyocytelike cells. Mol Med Rep. 2017; 16(5):6068-6076. https://doi.org/10.3892/mmr.2017.7333 PMid:28849052 PMCid:PMC5865810

31. Spitzhorn LS, Rahman MS, Schwindt L, Ho HT, Wruck W, Bohndorf M, Wehrmeyer S, Ncube A, Beyer I, Hagenbeck C et al. Isolation and Molecular Characterization of Amniotic Fluid-Derived Mesenchymal Stem Cells Obtained from Caesarean Sections. Stem Cells Int. 2017; 2017:5932706. https://doi.org/10.1155/2017/5932706 PMid:29225627 PMCid:PMC5684599

32. Zhou J, Wang D, Liang T, Guo Q, Zhang G. Amniotic fluid-derived mesenchymal stem cells: characteristics and therapeutic applications. Arch Gynecol Obstet. 2014; 290(2):223-231. https://doi.org/10.1007/s00404-014-3231-7 PMid:24744053

33. Savickiene J, Treigyte G, Baronaite S, Valiuliene G, Kaupinis A, Valius M, Arlauskiene A, Navakauskiene R. Human Amniotic Fluid Mesenchymal Stem Cells from Second- and Third-Trimester Amniocentesis: Differentiation Potential, Molecular Signature, and Proteome Analysis. Stem Cells Int. 2015; 2015:319238. https://doi.org/10.1155/2015/319238 PMid:26351462 PMCid:PMC4553339

34. Rodrigues MT, Lee BK, Lee SJ, Gomes ME, Reis RL, Atala A, Yoo JJ. The effect of differentiation stage of amniotic fluid stem cells on bone regeneration. Biomaterials. 2012; 33(26):6069-6078. https://doi.org/10.1016/j.biomaterials.2012.05.016 PMid:22672834

35. Olszta MJ, Cheng X, Jee SS, Kumar R, Kim YY, Kaufman MJ, Douglas EP, Gower LB. Bone structure and formation: A new perspective. Materials Science and Engineering. 2007; R 58:77-116. https://doi.org/10.1016/j.mser.2007.05.001

36. Guillaume O, Geven MA, Sprecher CM, Stadelmann VA, Grijpma DW, Tang TT, Qin L, Lai Y, Alini M, de Bruijn JD et al. Surface-enrichment with hydroxyapatite nanoparticles in stereolithography-fabricated composite polymer scaffolds promotes bone repair. Acta Biomater. 2017; 54:386-398. https://doi.org/10.1016/j.actbio.2017.03.006 PMid:28286037

37. Hossan MDJ, Gafur MA, Kadir MR, Karim MM. Preparation and Characterization of Gelatin-Hydroxyapatite Composite for Bone Tissue Engineering. International Journal of Engineering & Technology IJET-IJENS. 2014; 14(1). https://doi.org/10.3329/bjsir.v50i1.23805

38. Wei J, Jia J, Wu F, Wei S, Zhou H, Zhang H, Shin JW, Liu C. Hierarchically microporous/macroporous scaffold of magnesium-calcium phosphate for bone tissue regeneration. Biomaterials. 2010; 31(6):1260-1269. https://doi.org/10.1016/j.biomaterials.2009.11.005 PMid:19931903

39. Filipowska J, Lewandowska-Lancucka J, Gilarska A, Niedzwiedzki L, Nowakowska M. In vitro osteogenic potential of collagen/chitosan-based hydrogels-silica particles hybrids in human bone marrow-derived mesenchymal stromal cell cultures. Int J Biol Macromol. 2018; 113:692-700. https://doi.org/10.1016/j.ijbiomac.2018.02.161 PMid:29525638

40. Sharma C, Dinda AK, Potdar PD, Chou CF, Mishra NC. Fabrication and characterization of novel nano-biocomposite scaffold of chitosan-gelatin-alginate-hydroxyapatite for bone tissue engineering. Mater Sci Eng C Mater Biol Appl. 2016; 64:416-427. https://doi.org/10.1016/j.msec.2016.03.060 PMid:27127072

41. Ruphuy G, Souto-Lopes M, Paiva D, Costa P, Rodrigues AE, Monteiro FJ, Salgado CL, Fernandes MH, Lopes JC, Dias MM et al. Supercritical CO2 assisted process for the production of high-purity and sterile nano-hydroxyapatite/chitosan hybrid scaffolds. J Biomed Mater Res B Appl Biomater. 2018; 106(3):965-975. https://doi.org/10.1002/jbm.b.33903 PMid:28470936